ELSEVIER

Biophysical Chemistry 90 (2001) 103–121

Biophysical Chemistry

www.elsevier.nl/locate/bpc

Acid- and base-induced conformational transitions of equinatoxin II

Nataša Poklar[a,*], Jens Völker[b], Gregor Anderluh[a], Peter Maček[a], Tigran V. Chalikian[c,1]

[a] *Biotechnical Faculty, University of Ljubljana, Jamnikarjeva 101, 1000 Ljubljana, Slovenia*
[b] *Department of Chemistry, Rutgers, The State University of New Jersey, Piscataway, NJ 08854-8087, USA*
[c] *Department of Pharmaceutical Sciences, Faculty of Pharmacy, University of Toronto, 19 Russell Street, Toronto, Ontario M5S 2S2, Canada*

Received 11 September 2000; received in revised form 14 December 2000; accepted 18 December 2000

Abstract

We have investigated the acid- and base-induced conformational transitions of equinatoxin II (EqTxII), a pore-forming protein, by a combination of CD-spectroscopy, ultrasonic velocimetry, high precision densimetry, viscometry, gel electrophoresis, and hemolytic activity assays. Between pH 7 and 2, EqTxII does not exhibit any significant structural changes. Below pH 2, EqTxII undergoes a native-to-partially unfolded transition with a concomitant loss of its rigid tertiary structure and the formation of a non-native secondary structure containing additional α-helix. The acid-induced denatured state of EqTxII exhibits a higher intrinsic viscosity and a lower adiabatic compressibility than the native state. Above 50°C, the acid-induced denatured state of EqTxII reversibly denatures to a more unfolded state as judged by the far UV CD spectrum of the protein. At alkaline pH, EqTxII undergoes two base-induced conformational transitions. The first transition occurs between pH 7 and 10 and results in a partial disruption of tertiary structure, while the secondary structure remains largely preserved. The second transition occurs between pH 11 and 13 and results in the complete loss of tertiary structure and the formation of a non-native, more α-helical secondary structure. The acid- and base-induced partially unfolded states of EqTxII form water-soluble oligomers at low salt, while at high salt (> 350 mM NaCl), the acid-induced denatured state precipitates. The hemolytic activity assay shows that the acid- and base-induced denatured states of EqTxII exhibit significantly reduced activity compared to the native state.

Keywords: Equinatoxin II; Pore-forming proteins; Conformational transitions; CD spectroscopy; Volume; Compressibility

[1] Also corresponding author. Tel.: +1-416-946-3715; fax: +1-416-978-8511.
E-mail address: chalikan@phm.utoronto.ca (T.V. Chalikian).
* Corresponding author. Tel.: +386-1-423-1161; fax: +386-1-256-6298.
E-mail address: natasa.poklar@uni-lj.si (N. Poklar).

0301-4622/01/$ - see front matter
PII: S0301-4622(01)00131-4

1. Introduction

Pore-forming peptides and proteins have been found in a wide range of organisms, including bacteria, plants, fungi, primitive metazoans, insects, and mammals. These toxins are mostly water-soluble and exert their toxic influence by interacting with and forming pores in lipid membranes of a target organism [1]. Sea anemones produce one or more cytolysins all belonging to a protein family called actinoporins. Equinatoxin II (EqTxII) from the sea anemone *Actinia equina* L. belongs to this family. This predominantly β-sheet protein consists of 179 amino acid residues and lacks cysteins. EqTxII is characterized by a molecular mass of 19.8 kDa and an isoelectric point, pI, of 10.5 [2,3]. An important feature of EqTxII is that 30% of its amino acid residues are ionizable (10 aspartic acids, 4 glutamic acids, 5 histidines, 11 tyrosines, 9 lysines, and 10 arginines) [4]. Consequently, strong dependences of the properties of EqTxII on the solution pH and ionic strength can be anticipated. In aqueous solutions at neutral pH, EqTxII assumes its native globular conformation with rigid tertiary structure. As revealed by our initial studies, in response to changes in temperature, pH, and lipid concentration and composition, EqTxII may alter its conformational state [3,5,6]. In particular, our spectroscopic (fluorescence, circular dichroism, and light absorbance spectroscopy) and calorimetric (differential scanning calorimetry) measurements have revealed that, at low pH and 100 mM NaCl, EqTxII adopts a molten globule-like conformation which lacks rigid tertiary structure but exhibits enhanced α-helical secondary structure [3].

Here, we further characterize the conformational transitions of EqTxII at acidic pH as a function of salt and temperature by employing, in addition to CD spectroscopy, volumetric and viscometric techniques. Also, we characterize the base-induced conformational transitions of EqTxII by CD spectroscopy. These studies are aimed at better understanding the role of conformational transitions of the toxin in modulating its functional activity. For this reason, we measure the hemolytic activity of the native and acid- and base-induced denatured states of EqTxII.

2. Materials and methods

2.1. Materials

Equinatoxin II (EqTxII) was isolated from sea anemone *Actinia equina* L. as previously described [2] and stored freeze-dried at −10°C. CsOH, NaOH, HCl, and NaCl were purchased from Sigma Chemical (St. Louis, MO). The protein was dissolved in triply distilled water rather than buffers to avoid the need to correct for volume and compressibility changes due to the ionization–neutralization equilibria of the buffer. The concentration of EqTxII was determined spectrophotometrically using an extinction coefficient, ε_{280}, of 1.87 cm^{-1} g^{-1} at 25°C determined by dry weight analysis. For all ultrasonic velocimetric, densimetric, and viscometric measurements reported here, EqTxII concentration was 0.5–0.7 g l^{-1} (~25–35 μM), while the protein concentration for CD spectroscopic and native PAGE electrophoretic measurements was lower and equal to 0.3 g l^{-1} (~15 μM).

2.2. Methods

2.2.1. Ultrasonic velocimetry

Solution sound velocity measurements were performed at 7.5 MHz using the previously described resonator method [7–9]. We used an ultrasonic resonator cell with lithium niobate piezotransducers and a minimum sample volume of 0.8 cm^3 [8]. For this type of acoustic resonator, the relative precision of sound velocity measurements at frequencies near 7.5 MHz is at least $\pm 1 \times 10^{-4}$% [10,11].

The key characteristics of a solute directly derived from ultrasonic measurements is the relative specific sound velocity increment, $[u]$, which is equal to $(u - u_o)/(u_o c)$, where c is the specific concentration of a solute, and u and u_o are the sound velocities in the solution and the solvent, respectively. Acoustic pH titration experiments

were performed by addition of equal amounts of HCl solution to both the sample and reference cells each containing 1 cm^3 of the protein solution and water, respectively. The initial volume of 1 cm^3 was delivered to each cell by a 1-ml Hamilton syringe, while titrant solution were added by a 10-μl Hamilton syringe (Hamilton Co., Reno, NV). Each syringe was equipped with a Chaney adapter that allowed a relative delivery accuracy of $\pm 0.1\%$. When calculating the relative specific sound velocity increment, $[u]$, of EqTxII we took into account changes in the sound velocity in the solvent, u_o, and the specific concentration of the solute, c, which result from addition of the titrant.

2.2.2. High precision densimetry

All densities were measured at 25°C with a precision of $\pm 1.5 \times 10^{-6}$ g cm^{-3} using a vibrating tube densimeter (DMA-60/602, Anton Paar, Austria). We calculated the apparent specific volume, φv, of EqTxII using the well-known relationship [12]:

$$\varphi v = 1/\rho_o - (\rho - \rho_o)/(\rho_o c) \quad (1)$$

where ρ and ρ_o are the densities of the solution and the solvent, respectively.

Densimetric pH titration was carried out in a specially designed vial as previously described [13]. In calculating the apparent specific volume, φv, by means of Eq. (1), we took into account the changes in the solvent density, ρ_o, and the concentration of the solute, c, that result from addition of the titrant.

2.2.3. Determination of the apparent specific adiabatic compressibility

The relative specific sound velocity increments, $[u]$, determined as described above, were used in conjunction with our measured apparent specific volume data, φv, to calculate the apparent specific adiabatic compressibility, φk_S, of EqTxII using the following relationship [14]:

$$\varphi k_S = \beta_{So}(2\varphi v - 2[u] - 1/\rho_o) \quad (2)$$

where β_{So} is the coefficient of adiabatic compressibility of the solvent.

Each densimetric or ultrasonic velocimetric titration experiment was repeated two to three times, with the average values of $[u]$ and φv being used to calculate φk_S from Eq. (2).

2.2.4. Viscometry

Viscosity measurements were performed using an Ubbelohde Micro-Viscometers (Schott Glaswerke, Mainz, Germany) at a temperature of 25.00 ± 0.02°C controlled by a Heto model 01 PT 623 temperature bath (Birkerød, Denmark). The viscometer was filled with 2.5 ml of triply distilled water or the protein solution and titrated with HCl or NaOH. The protein dilution after each titration did not exceed 10%. The relative viscosity, η_{rel}, of the protein solution was calculated as $\eta_{rel} = \eta/\eta_o = \rho t/\rho_o t_o$, where t and t_o are the flow times for the solution and the solvent, respectively; ρ and ρ_o are densities of the solution and the solvent, respectively. The intrinsic viscosity, $[\eta]$, of EqTxII was calculated by dividing the specific viscosity ($\eta_{sp} = \eta_{rel} - 1$), by the protein concentration, η_{sp}/c.

2.2.5. Circular dichroism spectroscopy

All circular dichroism (CD) spectra of EqTxII were recorded using an AVIV model 62A DS Spectropolarimeter (Aviv Associates, Lakewood, NJ). The far UV (200–250 nm) and near UV (250–300 nm) CD spectra of EqTx II were measured using 1- and 10-mm path length quartz cuvettes, respectively.

2.2.6. Native gel electrophoresis

Native polyacrylamide gel electrophoresis (PAGE) was performed in a PHAST System (Amersham Pharmacia Biotech, Uppsala, Sweden) using 20% gels and reverse electrodes according to instructions of the manufacturer. Each sample was diluted with an equal volume of sample buffer (0.224 M Tris–HCl, 0.224 M sodium acetate, pH 6.4, crystal violet as a tracking dye) and applied to the gel. After electrophoresis, gels were silver-stained and documented using a UVItec documentation system (UVItec Limited, Cambridge, England). Bands on the gel were quantified using the UVIPhoto software from the same manufacturer.

2.2.7. Hemolytic activity

The hemolytic activity of EqTxII was measured turbidimetrically on bovine red blood cells (BRBC) at 25°C using a microplate reader (MRX, Dynex Technologies, Denkendorf, Germany) as described previously [15].

2.2.8. pH measurements

The pH of all protein solutions were measured separately for each experiment using a VWR model 8015 pH-meter and an Accumet Ag/AgCl combination microelectrode. Absolute error of our pH measurements was ± 0.01 pH units.

3. Results

3.1. CD-spectroscopy

Fig. 1 presents the near UV (panel a) and far UV (panel b) CD spectra of EqTxII recorded between pH 6 and 1 at 25°C in the absence of salt. For comparison, Fig. 1 also shows the near UV (panel a) and far UV (panel b) CD spectra of the fully unfolded state of EqTxII in 5 M GuHCl at pH 0.5 and 25°C. To examine the effects of salt and temperature on the acid-induced denatured state of EqTxII, we have measured the far UV CD spectra of the protein at different temperatures and salt concentrations. Fig. 2 presents the far UV CD spectra of the protein at temperatures between 5°C and 95°C at pH 1.2 in the absence of salt. As shown in Fig. 2, the far UV CD spectrum of the acid-induced denatured state of EqTxII becomes significantly altered at temperatures above 50°C. By contrast, judging by the far UV CD spectrum of the acid-induced denatured state of EqTxII at pH 1.2 and 25°C, the structure is practically unaffected by salt at NaCl concentrations of up to 350 mM (data not shown). However, at higher salt, the protein precipitates with a concomitant decrease in the CD signal due to a decrease in the concentration of the protein that remains in solution.

Fig. 3 shows the near UV (panel a) and far UV (panel b) CD spectra of EqTxII in the absence of salt in the pH range between pH 6 and 13.5 (25°C). For comparison, Fig. 3 also shows the near UV (panel a) and far UV (panel b) CD spectra of the fully unfolded state of EqTxII in 5 M GuHCl at pH 12 and 25°C. In our alkaline titration experiments, the solution pH was adjusted by addition of aliquots of CsOH. A comparative titration of EqTxII with NaOH (data not shown) resulted in CD spectra which were superimposable to those obtained from CsOH titration. To investigate the reversibility of the acid- and base-induced conformational transitions of EqTxII at 25°C, we performed reverse CD titrations of the denatured protein states by incremental additions of aliquots of CsOH (not shown) or HCl (see Fig. 4). Fig. 4 presents the far UV CD spectra of EqTxII at different pH when the solution pH was gradually reduced from highly alkaline (pH 13.3) to highly acidic (pH 1.3) values by titrating with HCl the solution of the base-induced denatured state of the protein. In general, our results reveal that the base-induced denaturation of EqTxII is partially reversible, while the acid-induced denaturation is irreversible. It should be noted that the base-induced denatured state of EqTxII at pH 13 and 25°C remains water-soluble at NaCl concentrations of up to 1 M.

The pH-induced conformational transitions of EqTxII can be monitored by plotting the molar ellipticity of the protein at selected wavelengths against the pH. Fig. 5a shows how the molar ellipticities of EqTxII in the near UV range (at 255 and 270 nm) change with pH. Fig. 5b presents similar dependencies for the far UV range (at 208 and 217 nm). Inspection of Fig. 5a,b reveals that the toxin undergoes an acid-induced conformational transition below pH 2 and two base-induced conformational transitions, one between pH 7 and 10 and the other between pH 11 and 13.

3.2. Sound velocity, volume, and compressibility

In this paper, we report volumetric data for EqTxII only at acidic pH (between pH 6 and 1). At alkaline pH, volumetric measurements of EqTxII solutions become complicated due to a sharp decrease in the solubility of the protein near its isoelectric point (pI 10.5). Fig. 6 shows the pH-dependences of the partial specific volume, v^o (panel a), relative specific sound velocity incre-

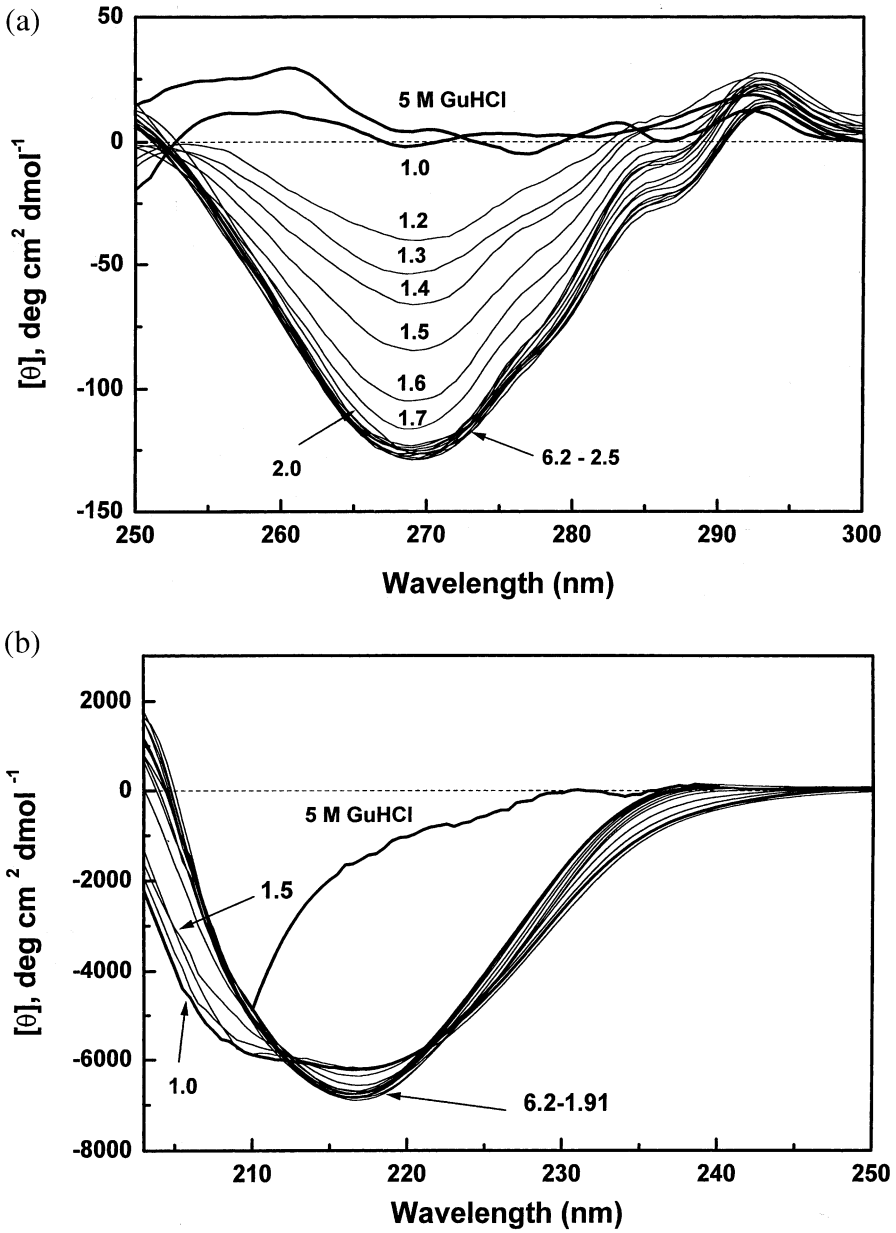

Fig. 1. CD spectra of EqTxII in the acidic pH range at 25°C. (a) Near UV; (b) far UV.

ment, $[u]$ (panel b), and partial specific adiabatic compressibility, k_S^o (panel c), of EqTxII at 25°C in the absence of salt. Errors were estimated by taking into account uncertainties due to concentration determinations, temperature drifts, and inherent instrument characteristics. Strictly speaking, the data in Fig. 6a,c correspond to the apparent specific volume, φv, and adiabatic compressibility, φk_S, of EqTxII. However, for globular proteins, the concentration dependences of φv and φk_S are known to be weak [16,17]. Therefore, within the limits of experimental error, our data

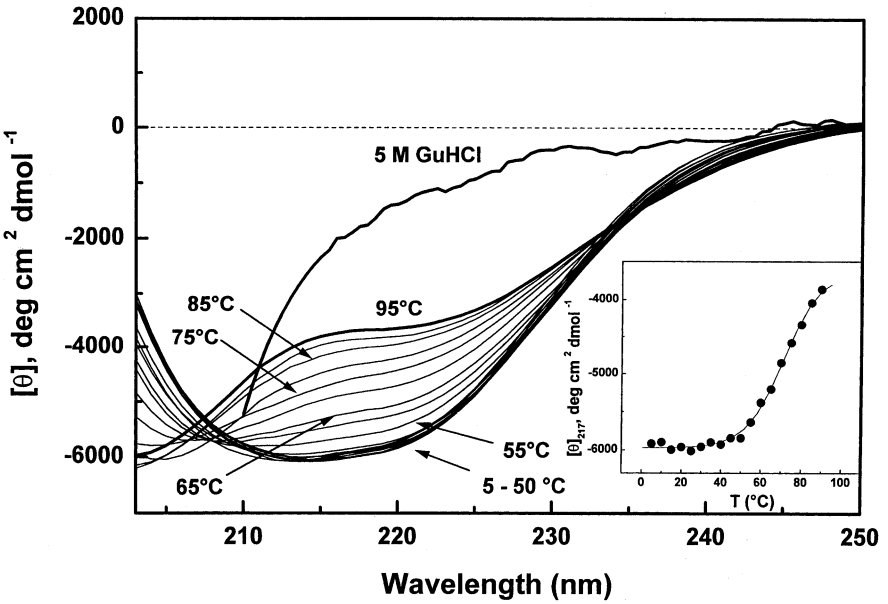

Fig. 2. Temperature dependence of EqTxII CD spectra at pH 1.2 and 25°C. Insert: temperature dependence of the molar ellipticity at 217 nm.

determined at protein concentrations of 0.5–0.7 g l^{-1} correspond to the partial specific volume, v^{o}, and adiabatic compressibility, k_S^o, of EqTxII obtained by extrapolation to infinite dilution. Consequently, in our analysis below, we do not discriminate between the partial and apparent specific values.

Inspection of Fig. 6a reveals that, at pH 6, EqTxII exhibits a partial specific volume of (0.767 $\pm$ 0.005) cm^3 g^{-1} which is slightly larger than the values reported for other globular proteins in their native state at 25°C [16,18]. Further inspection of Fig. 6a reveals that, within our experimental uncertainty of ± 0.01 cm^3 g^{-1}, a decrease in pH from neutral to very acidic values does not cause any appreciable change in v^{o}. By contrast, inspection of Fig. 6b reveals that the relative specific sound velocity increment, $[u]$, of EqTxII strongly depends on pH. The value of $[u]$ remains essentially constant between pH 2 and 6, while increasing below pH 2. At neutral pH, the relative specific sound velocity increment, $[u]$, of EqTxII is equal to 0.159 ± 0.003 cm^3 g^{-1}, a value typical for globular proteins [16–18].

At neutral pH, the partial specific adiabatic compressibility, k_S^o, of the protein is $(9.1 \pm 0.7) \times 10^{-6}$ cm^3 g^{-1} bar^{-1} (see Fig. 6c) which corresponds to the upper range of k_S^o values reported for other globular proteins [16–18]. Inspection of Fig. 6c reveals the presence of small changes in k_S^o around pH 2.5 and pH 4.5 which, most probably, are related to the neutralization of titrable groups of EqTxII without global disruption of the protein conformation. Between pH 2 and 1, k_S^o steadily decreases and does not level off even at pH 1, our lowest experimental pH. This observation suggests that the acid-induced denaturation of EqTxII is not complete at pH 1. At this pH, the value of k_S^o is roughly equal to 6×10^{-6} cm^3 g^{-1} bar^{-1}.

3.3. Viscosity

Analogous to the volumetric measurements, our viscosity data on EqTxII have been collected only at acidic pH, since the protein solubility sharply decreases at alkaline pH. Recall that the viscosity of a protein solution reflects the shape and rela-

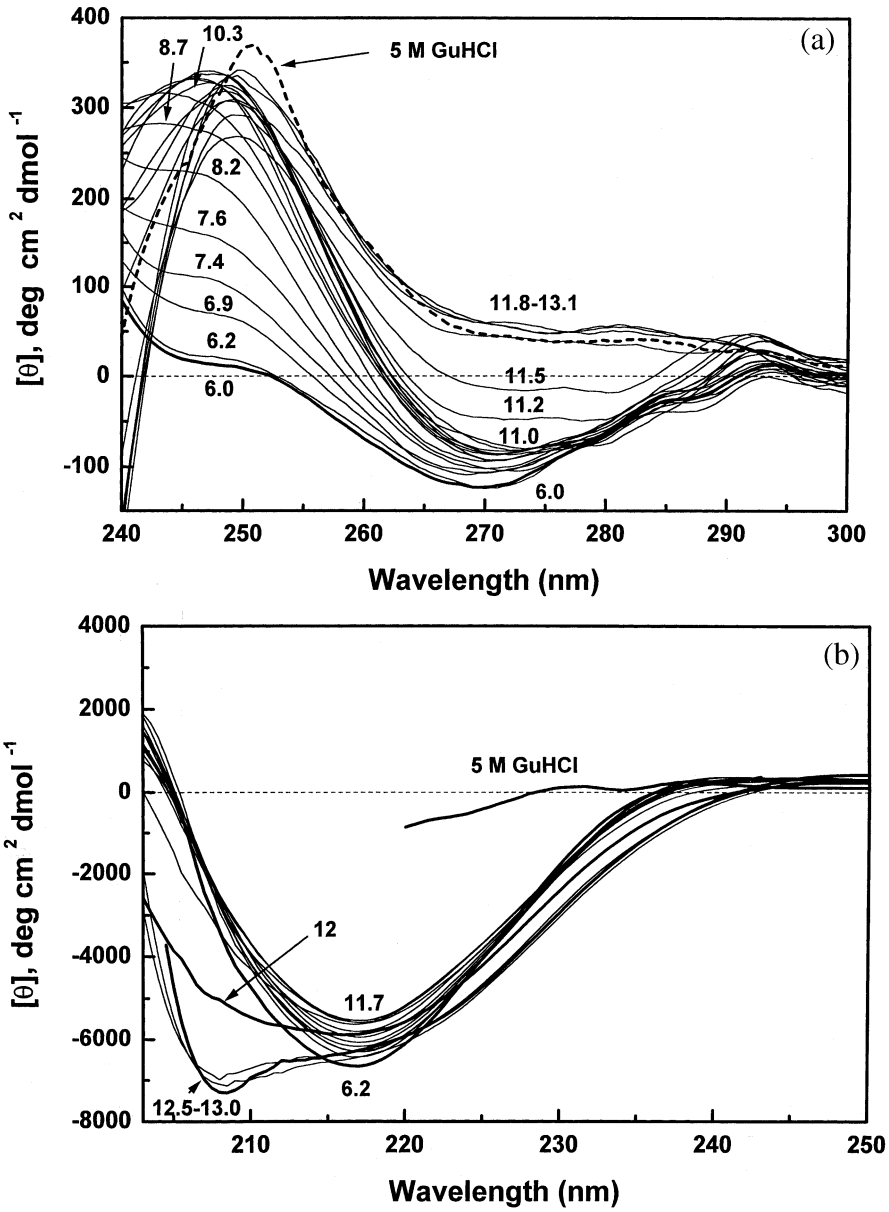

Fig. 3. CD spectra of EqTxII in the alkaline pH range at 25°C. (a) Near UV; (b) far UV.

tive size of protein molecules. Consequently, viscosity measurements provide a useful tool for detecting changes in protein compactness induced by conformational transitions [19]. Fig. 7 shows the intrinsic viscosity of EqTxII, [η], as a function of pH at 25°C. Errors were estimated by taking into account uncertainties due to concentration determinations, temperature drifts, and inherent instrument characteristics. Inspection of Fig. 7 reveals that, between pH 6 and 2, the value of [η] is practically pH-independent. Below pH 2, the intrinsic viscosity, [η], of the protein increases

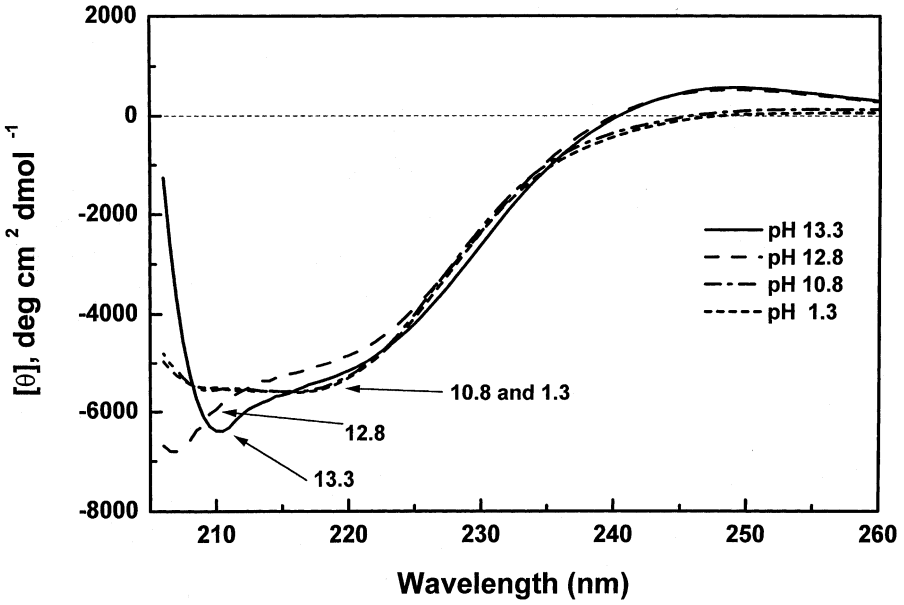

Fig. 4. CD spectra at 25°C of EqTxII upon reverse titration of the base-induced denatured form.

from 0.01 to 0.03 $cm^3\ g^{-1}$ at pH 1, but does not level off even at this lowest experimental pH. At pH 1, the value of [η] is only a half the value of [η] in 5 M GuHCl at pH 0.5 and 25°C. However, one cannot exclude the possibility that, upon completion of the acid-induced denaturation of EqTxII at lower pH, the value of [η] would approach that of the fully unfolded state in 5 M GuHCl.

3.4. Native-PAGE

Fig. 8 presents the results of our native PAGE electrophoresis experiments of EqTxII after treatment with pH and/or temperature. In general, depending on the conformational state, the toxin can be monomeric or oligomeric. At pH 5.5 and 25°C, EqTxII exists in its native monomeric form. After incubation at pH 5.5 and 95°C for 30 min and storage at 25°C overnight, the protein is only partially monomeric (15%), while the rest of the protein forms high molecular weight, water-soluble aggregates. At pH 1.2 (at 25°C and 95°C) and 12.6 (at 25°C), EqTxII oligomerizes and forms high molecular weight, water-soluble aggregates. These aggregates are so large that they cannot enter the resolving gel and remain at the border between the stacking and resolving gels. In some cases, the aggregates even remain within the loading wells without penetrating into the stacking gel at all (e.g. at pH 12.6 and 25°C or pH 5.5 and 95°C). No protein band was observed on the gel after incubation of EqTxII at pH 12.6 and 95°C suggesting extensive hydrolysis of the protein.

3.5. Hemolytic activity

Hemolysis of bovine red blood cells is a sensitive assay, which has been widely used in functional studies of actinoporins and other pore-forming toxins [20]. Any structural change of EqTxII induced by pH and temperature should alter its biological activity, which, in turn, should be reflected in the hemolytic function of the toxin. Fig. 9 shows the concentration dependencies of the rate of bovine red blood cell hemolysis

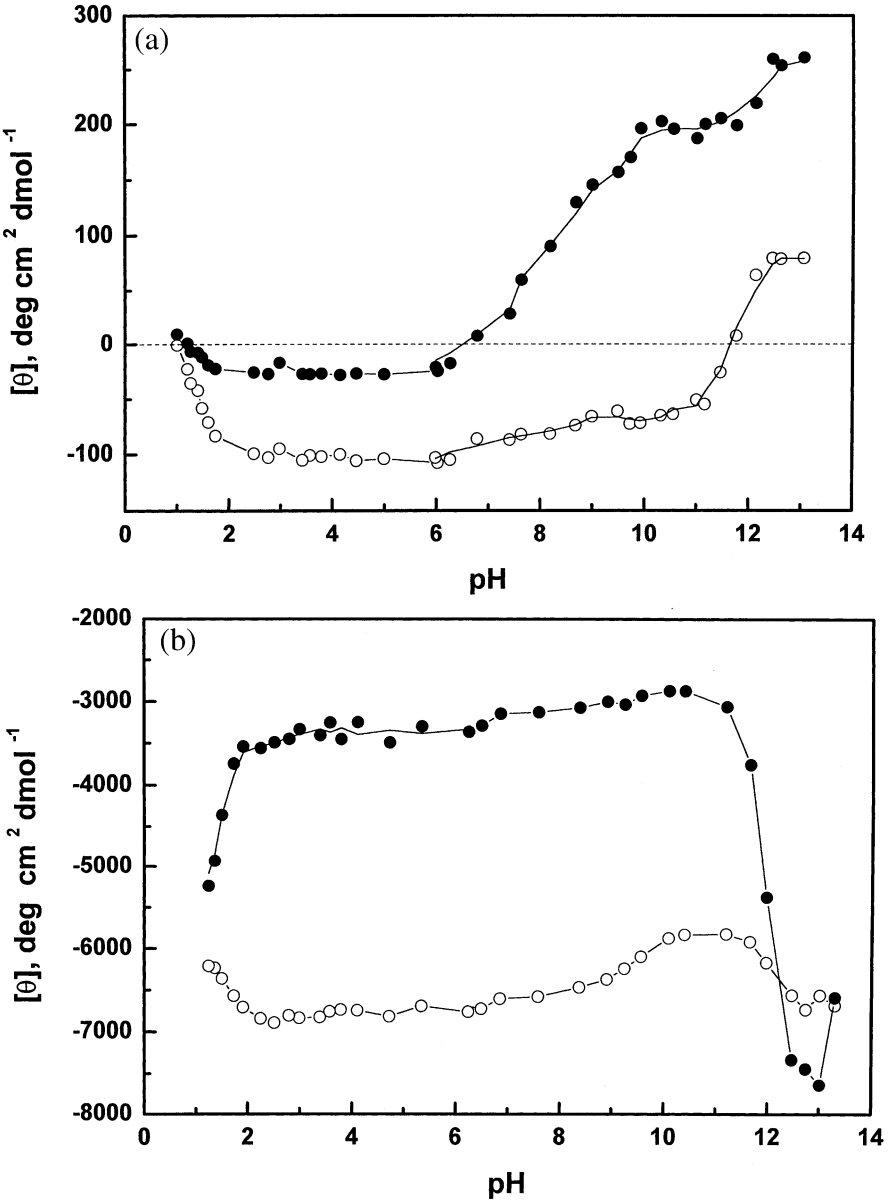

Fig. 5. The pH-dependences of EqTxII single wavelength molar ellipticities at 25°C. (a) Near UV, (●) 255 nm and (○) 270 nm. (b) Far UV, (●) 208 nm and (○) 217 nm.

in erythrocyte buffer (0.13 M NaCl, 0.02 M Tris–HCl, pH 7.4) for EqTxII preincubated at different environmental conditions. Errors were estimated as the standard errors of the mean. Inspection of Fig. 9 reveals that EqTxII incubated at pH 5.5 and 95°C for 30 min and stored at 25°C overnight maintains only 48% of the original hemolytic activity. Incubation of the toxin at pH 1.2, regardless of the incubation temperature and salt, reduces the hemolytic activity by, at least,

two orders of magnitude. Incubation of the toxin at pH 12.6 and 25°C causes a reduction in the hemolytic activity of the protein by an additional order of magnitude. Finally, samples of EqTxII, which were incubated for any length of time at pH 12.6 and 95°C, completely lose their functional activity. The lack of hemolytic activity at pH 12.6 and 95°C is in good agreement with the

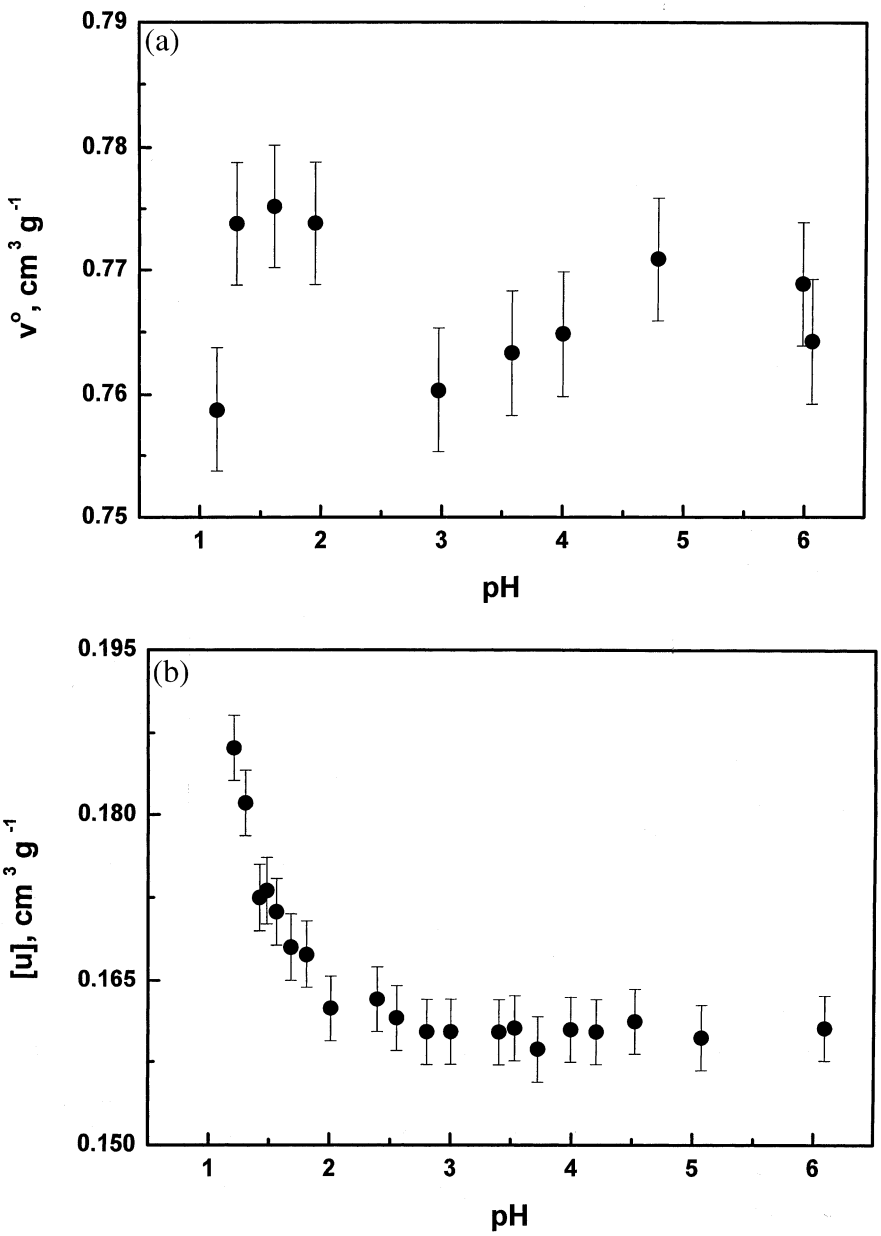

Fig. 6. The pH-dependences for EqTxII at 25°C of the partial specific volume (a), relative specific sound velocity increment (b), and partial specific adiabatic compressibility (c).

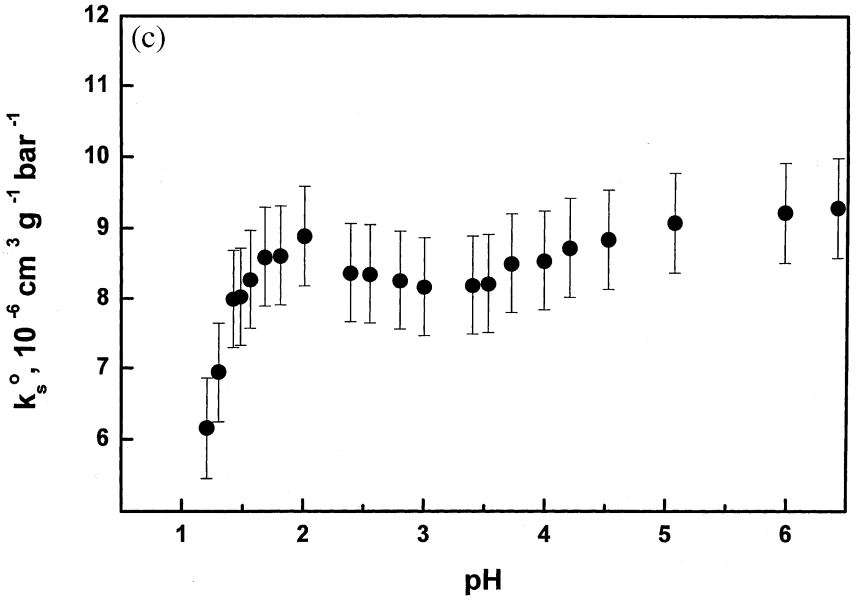

Fig. 6. (Continued).

absence of protein bands on the native gel, consistent with extensive hydrolysis of the protein under these harsh denaturing conditions.

4. Discussion

4.1. Acid-induced denaturation of EqTxII

4.1.1. CD spectroscopy

Inspection of Fig. 1a,b reveals the absence of any significant changes in tertiary and secondary structures of EqTxII between pH 6 and 2. This observation is consistent with our ultrasonic velocimetric and viscometric results (see Fig. 6a and Fig. 7). However, below pH 2, the protein loses its native conformation. Specifically, the near UV CD spectrum of EqTxII begins to decrease in intensity and, around pH 1, becomes indistinguishable from that of the toxin in 5 M GuHCl at pH 0.5 and 25°C (see Fig. 1a). Similarly, judging by the far UV CD spectra of EqTxII presented in Fig. 1b, the secondary structure of the protein begins to change below pH 2. The far UV CD spectrum of EqTxII near pH 1, with two distinguishable minima at 208 and 220 nm, is distinct from that of the native protein at neutral pH, which has only a single minimum at 217 nm. Importantly, the far UV CD spectrum of the acid-induced denatured state of EqTxII at around pH 1 differs qualitatively and quantitatively from that of the fully unfolded state of the protein in 5 M GuHCl at pH 0.5 and 25°C. Using a secondary structure deconvolution algorithm [21,22], we estimate that, above pH 2, EqTxII is a predominantly β-sheet protein. Specifically, at pH 6, EqTxII has $12 \pm 1\%$ α-helical structure, $52 \pm 5\%$ β-structure, and $36 \pm 3\%$ aperiodic secondary structure. By contrast, the shape of the far UV CD spectrum of EqTxII near pH 1 suggests a higher content of α-helical secondary structure of at least 19% [21,22]. Specifically, we find that, at pH 1.2, EqTxII has $19 \pm 1\%$ α-helical structure, $46 \pm 5\%$ β-structure, and $35 \pm 4\%$ aperiodic secondary structure.

Taken together, these observations suggest that, between pH 2 and 1, EqTxII undergoes a conformational transition to a denatured state, which lacks rigid tertiary structure but exhibits en-

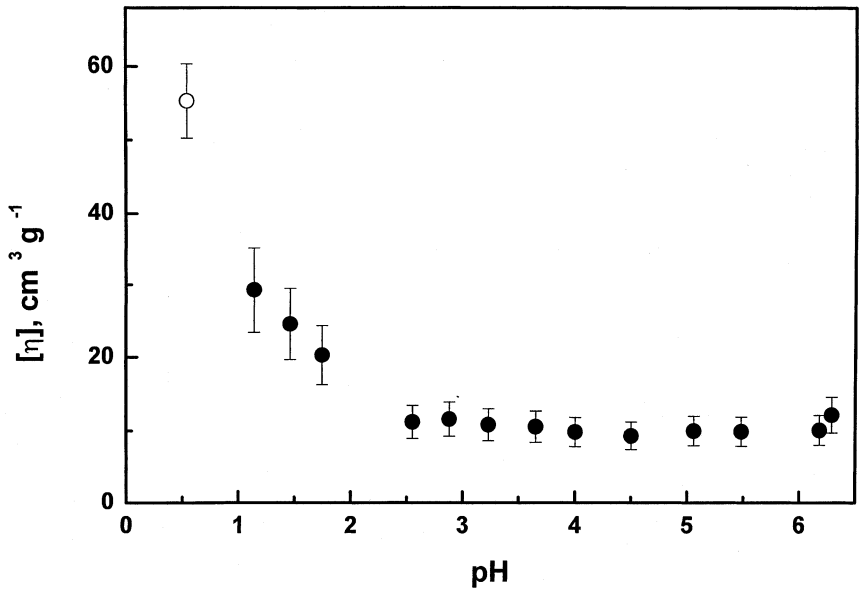

Fig. 7. The pH-dependence of the intrinsic viscosity of EqTxII at 25°C in 0 M (●) and 5 M (○) GuHCl.

hanced α-helical secondary structure. This transition can be followed by the ellipticity-vs.-pH profiles depicted in Fig. 5a,b. Significantly, inspection of the four curves in Fig. 5a,b reveals that the acid-induced denaturation of EqTxII is not complete even at pH 1, our lowest experimental pH. Recall that we arrived at a similar conclusion based on our ultrasonic velocimetric and viscometric data.

As is seen from Fig. 1a,b, both the near UV and far UV CD spectra of EqTxII contain isodichroic points: near 212, 222 (far UV), and 252 (near UV) nm. The slight deviations from rigorously isodichroic points are, probably, due to small inaccuracies in protein concentration measurements, in dispensing the protein and titrant solutions, or a combination of both. All three isodichroic points occur between pH 2 and 1, suggesting the existence of two spectroscopic states in this pH range. Based on this observation,

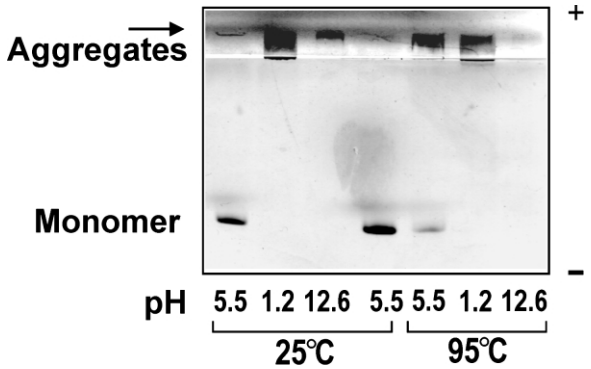

Fig. 8. Native PAGE electrophoretograms of EqTxII preincubated at different conditions as marked.

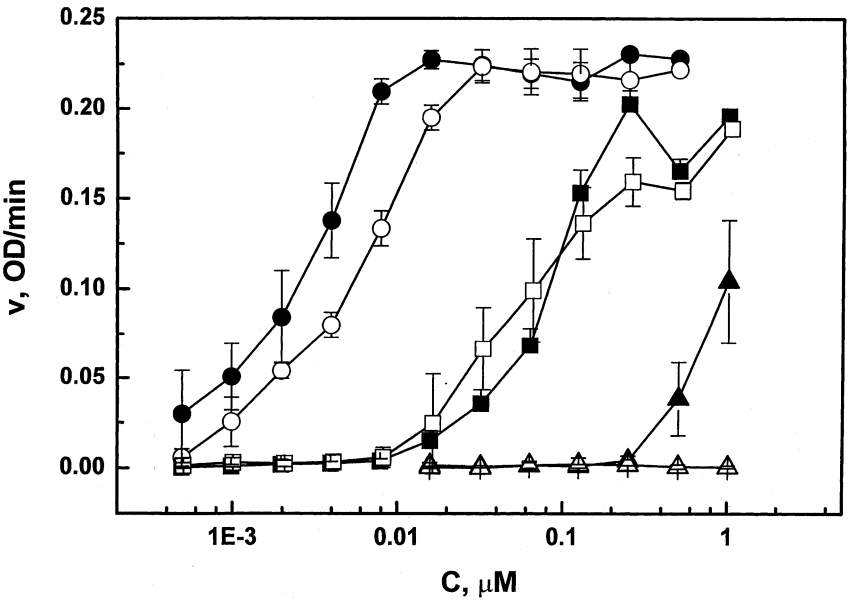

Fig. 9. The rate of hemolysis of bovine red blood cells by EqTxII as a function of toxin concentration. EqTxII was preincubated at pH 5.5 and 25°C (●); pH 1.2 and 25°C (■); pH 12.6 and 25°C (▲); pH 5.5 and 95°C (○); pH 1.2 and 95°C (□); and pH 12.6 and 95°C (△).

we conclude that the acid-induced conformational transition of EqTxII is consistent with a two-state transition.

Inspection of Fig. 2 reveals that the far UV CD spectrum of the protein at pH 1.2 remains essentially the same at temperatures up to 50°C. Above 50°C, the acid-induced denatured state of EqTxII reversibly converts into a more unfolded state with less ordered secondary structure, as revealed by an increase in molar ellipticity between 210 and 230 nm. The latter state, however, remains distinct from the fully unfolded state of EqTxII in 5 M GuHCl at pH 0.5 and 25°C. Note that the insert in Fig. 2 (the molar ellipticity of EqTxII at 217 nm as a function of temperature) has the shape of a classical, cooperative two-state transition. This observation is consistent with the two isodichroic points in the main part of Fig. 2: one near 208 nm and another near 235 nm. The deviation from perfect isodichroity in these experiments could arise from the technical reasons mentioned above as well as from concentration inaccuracies owing to solvent evaporation at elevated temperatures. Thus, we conclude that, at pH 1.2, EqTxII undergoes a heat-induced reversible two-state-like transition into a state with more disordered secondary structure. Based on the far UV CD spectrum of EqTxII, we estimate that, at pH 1.2 and 95°C, the toxin still contains approximately $7 \pm 2\%$ α-helical structure and $38 \pm 4\%$ β-structure while the fraction of aperiodic structure is only $55 \pm 2\%$. Judging by the fraction of unordered secondary structure, the conformational state of EqTxII at pH 1.2 and 95°C cannot be described as fully unfolded. Given the cooperative nature of the heat-induced unfolding of the acid-induced denatured state of EqTxII, one can speculate that the latter state represents a 'non-compact' intermediate state of the protein. One can speculate even further that this equilibrium intermediate may resemble some kinetic intermediate on the EqTxII folding pathway. Clearly, further studies are needed to prove or refute these proposals/speculations.

4.1.2. Volume and compressibility

Volumetric observables such as partial specific volume and adiabatic compressibility provide in-

formation about the hydration properties and intrinsic packing of biological molecules [23–25]. With respect to proteins, compressibility measurements can also be used as a probe for protein conformation [25–27].

In general, changes in volume, Δv, and compressibility, Δk_S, associated with the acid-induced denaturation of a protein can be presented as a sum of 'conformational' and 'protonation' contributions [13,28]:

$$\Delta v = \Delta v_{conf} + \Delta v_{prot} \quad (3)$$

$$\Delta k_S = \Delta k_{Sconf} + \Delta k_{Sprot} \quad (4)$$

where Δv_{conf} and Δk_{Sconf} represent the pH-independent conformational changes in the volume and compressibility of a protein. Note that Δv_{conf} and Δk_{Sconf} represent the difference in the partial specific volume and adiabatic compressibility between the denatured and native states of a protein at the same pH; Δv_{prot} and Δk_{Sprot} represent the pH-dependent changes in the protein volume and compressibility due to protonation of titrable groups which may or may not cause global disruption of protein structure. Strictly speaking, Eq. (4) should also contain a pH-dependent relaxation term, Δk_{Srel}, which represents the change in protein compressibility due to proton-transfer-induced ultrasonic relaxation [29–31]. However, in our analysis below, the relaxation term, Δk_{Srel}, is neglected since its contribution to the value of Δk_S in Eq. (4) is rather small for acid-induced protein transitions [28,29]. In addition, ultrasonic relaxation associated with proton-transfer reactions reaches its maximum around the pK_a of titrable groups (between pH 3 and 4) and essentially subsides to zero below pH 2 [30].

The protonation terms, Δv_{prot} and Δk_{Sprot}, in Eqs. (3) and (4) reflect the changes in the hydration of ionizable groups upon their protonation. Recall that EqTxII has 10 Asp residues, four Glu residues, five His residues, and the C-terminal carboxyl group that become protonated when the solution pH decreases from pH 6 to 1. To account for the protonation-induced changes in protein volume and compressibility, Δv_{prot} and Δk_{Sprot}, we model the protonation of the titrable groups of EqTxII by the protonation of the carboxyl and amino termini of triglycine [32]. We have recently discussed advantages and disadvantages of using triglycine as a model system for mimicking the hydration properties of protein ionizable groups [28]. In short, we assign to the protonation of each Asp and Glu residue and the C-terminal carboxyl group the changes in volume and compressibility equal to 10.5 $cm^3\ mol^{-1}$ and $18.4 \times 10^{-4}\ cm^3\ mol^{-1}\ bar^{-1}$, respectively [28]. Furthermore, we assign to the protonation of each His residue the changes in volume and compressibility of $-4.5\ cm^3\ mol^{-1}$ and $-18.5 \times 10^{-4}\ cm^3\ mol^{-1}\ bar^{-1}$, respectively [28]. It is reasonable to assume that only one-half of the His residues of EqTxII become protonated below pH 6 since the pK_a of His is 6. With these assumptions, we calculate Δv_{prot} and Δk_{Sprot} in Eqs. (3) and (4) to be equal to 0.007 $cm^3\ g^{-1}$ $[(15 \times 10.5 - 0.5 \times 5 \times 4.5)/19\,800]$ and $1.2 \times 10^{-6}\ cm^3\ g^{-1}\ bar^{-1}$ $[(15 \times 18.4 \times 10^{-4} - 0.5 \times 5 \times 18.5 \times 10^{-4})/19\,800]$, respectively.

Inspection of Fig. 6a reveals that a decrease in the solution pH from pH 6 to 1 causes no appreciable change in the partial specific volume, v^o, of EqTxII. Our calculated value of Δv_{prot}, of 0.007 $cm^3\ g^{-1}$ is within the experimental error of $\pm 0.01\ cm^3\ g^{-1}$. Consequently, based on Eq. (3), we conclude that the value of Δv_{conf} for the acid-induced denaturation of EqTxII is essentially zero within the experimental uncertainty of $\pm 0.01\ cm^3\ g^{-1}$. This result is in agreement with previous thermodynamic studies on proteins which have reported only small, positive or negative, volume changes associated with conformational transitions of proteins [25,27,33]. It is worth mentioning that these small magnitude of the denaturation volume for a globular protein results from a compensation between different contributions to its partial specific volume [25,27,33]. In particular, we have recently suggested that the near zero volume changes observed for small globular proteins reflect fortuitous compensations between the negative contributions of enhanced hydration and reduced intramolecular void volume and the positive contribution of the thermal volume (which

results from the thermally-induced mutual motions of solute and solvent molecules) [27].

Inspection of Fig. 6c reveals that the partial specific adiabatic compressibility, k_S^o, of EqTxII diminishes by 3.5×10^{-6} cm^3 g^{-1} bar^{-1} upon a decrease in the pH from pH 6 to 1. Since, Δk_{Sprot} in Eq. (4) is 1.2×10^{-6} cm^3 g^{-1} bar^{-1}, the value of Δk_{Sconf} for the acid-induced unfolding of EqTxII can be calculated to be -4.7×10^{-6} cm^3 g^{-1} bar^{-1} ($-3.5 \times 10^{-6} - 1.2 \times 10^{-6}$). However, as discussed in the previous section, the acid-induced denaturation of EqTxII is not complete even at pH 1. Consequently, the real value of Δk_{Sconf} should be even more negative. If we arbitrarily assume (based on our rough evaluation of the denaturation profiles in Fig. 5) that, at pH 1, the protein denaturation is 50% complete, then the real value of Δk_{Sconf} is roughly equal to -9.5×10^{-6} cm^3 g^{-1} bar^{-1} [$2 \times (-4.7 \times 10^{-6})$].

For globular proteins, the partial specific adiabatic compressibility, k_S^o, is the sum of a positive intrinsic contribution, k_M, and a negative hydration contribution, Δk_h [16–18,23–26]. The intrinsic contribution, k_M, of a globular protein results from the imperfect packing of the polypeptide chain(s) within the solvent inaccessible interior. The hydration contribution, Δk_h, reflects the decrease in the solvent compressibility which results from interactions between the surface atomic groups of the protein and the surrounding water molecules. A 9.5×10^{-6} cm^3 g^{-1} bar^{-1} decrease in compressibility associated with the acid-induced denaturation of EqTxII reflects significant reductions in both the intrinsic, k_M, and hydration, Δk_h, contributions to k_S^o. In this respect, it should be noted that, for small globular proteins, the change in adiabatic compressibility, k_S^o, correlates with the type of transition being monitored, independent of the specific protein [26]. Specifically, native-to-molten globule state transitions result in small increases in compressibility, k_S^o (1×10^{-6} to 4×10^{-6} cm^3 g^{-1} bar^{-1}), native-to-partially unfolded state transitions are accompanied by small decreases in k_S^o (-3×10^{-6} to -7×10^{-6} cm^3 g^{-1} bar^{-1}), while native-to-fully unfolded transitions cause large decreases in k_S^o (-18×10^{-6} to -20×10^{-6} cm^3 g^{-1} bar^{-1}). According to this compressibility scale, the acid-induced denatured state of EqTxII with Δk_S^o of $\sim -9.5 \times 10^{-6}$ cm^3 g^{-1} bar^{-1} is closer to the range of compressibility changes characteristic for the ensemble of partially unfolded protein states. Partially unfolded proteins lack compactness and native secondary and tertiary structures while retaining some solvent-inaccessible, mostly hydrophobic core. Concomitantly, the partially unfolded state of a globular protein is characterized by significantly enhanced hydration compared to its compact native state. This interpretation is in qualitative agreement with our spectroscopic and viscometric results (see Fig. 7), which suggest, that, below pH 2, the protein adopts an essentially expanded conformation with disrupted tertiary structure and non-native α-helical secondary structure. A similar acid-induced formation of non-native α-helical secondary structure has been observed earlier for other β-sheet proteins, such as tumor necrosis factor-α [34] and cardiotoxin analogue III [35].

4.1.3. Oligomerization of the acid-induced denatured state of EqTxII

Denatured states of proteins tend to aggregate either reversibly or irreversibly [36–40]. Recall that our native-PAGE results (see Fig. 8) reveal that, at 25°C, EqTxII oligomerizes near pH 1 and forms large water-soluble aggregates. Such an association of denatured protein molecules may, in turn, facilitate formation of α-helical secondary structure as has been observed by Uversky et al. [41,42] for the acid-induced denatured states of staphylococcal nuclease. Thus, the formation of non-native α-helical secondary structure in the acid-induced denatured state of EqTxII may, in part, result from protein aggregation. On the other hand, aggregation of the acid-induced denatured state of EqTxII should cause a significant reduction of protein hydration with a concomitant increase in the negative hydration contribution to k_S^o [18]. Consequently, the 'true' change in adiabatic compressibility, Δk_S^o, associated with the acid-induced denaturation of an isolated EqTxII molecule is, probably, more negative than our estimate of $\sim -9.5 \times 10^{-6}$ cm^3 g^{-1} bar^{-1}.

A similar association of protein monomers has

been reported for melittin, a pore-forming peptide, which exhibits some sequence homology with the N-terminal domain of EqTxII [4]. A reduction of the net charge of melittin by pH, acetylation, succinylation, or salt facilitates formation of tetrameric, α-helix enriched structure [43]. Another β-sheet protein, tumor necrosis factor-α (TNF-α) converts at acidic pH into a monomeric form with enhanced α-helical content. This novel α-helical structure is not observed in the native trimeric form of the protein and has characteristics of a molten globule. It is worth noting that TNF-α can adopt at least two different acid-induced denatured states: a monomeric form in the absence of salt and an oligomeric, less α-helical form at high salt [34].

4.2. Base-induced denaturation of EqTxII

4.2.1. CD spectroscopy

Inspection of Fig. 3a and Fig. 5a reveals two base-induced spectral changes/transitions in the near UV range. The first transition starts near pH 7 and is accompanied by large changes in ellipticity between 240 and 260 nm and relatively small changes around 270 nm (see Fig. 3a). These CD spectral changes suggest that the first base-induced conformational transition of EqTxII (between pH 7 and 10) brings about some disruption of the native tertiary structure of the toxin. Alternatively, the change in ellipticity between 240 and 260 nm around pH 7 may arise from what appear to be small changes in the far UV CD spectrum in Fig. 3b. Recall that the far UV ellipticity bands are mainly due to the peptide chromophores. Compared to the side chain bands in the near UV, the peptide bands in the far UV are intensive, having 10 times the near UV ellipticities (note the ordinate scales on Fig. 3a,b). The far UV peptide bands overlap the near UV side chain bands in the 250-nm region. Consequently, small ellipticity changes in the far UV region (see Fig. 3b) due to minor secondary structural changes of the toxin near neutral pH will have strong effects on the short wavelength end of the near UV CD spectrum of EqTxII presented in Fig. 3a. Consistent with this line of reasoning, the observed rise in positive intensity and separation of the pH 6 shoulder at 250 nm (see Fig. 3a) into a more distinct band could easily come about if the far UV CD between 235 and 240 nm (see Fig. 3b) were to become less negative or were to shift to slightly shorter wavelengths or both. Clearly, further studies are required to clarify the nature of the CD structural changes around 250 nm observed between pH 7 and 10.

The second base-induced transition of EqTxII starts at pH 11 and is accompanied by significant changes in ellipticity around 270 nm and a red shift in the position of the positive maximum from 243 nm at pH 10.3 to 250 nm at pH 13.1 (see Fig. 3a). Significantly, this shift to longer wavelengths above pH 10.3 is accompanied first by a reduction in the ellipticity and then by an increase. The observed red shift can be accounted for by the ionization of solvent exposed tyrosine residues at pH 10 [44]. In general, the near UV CD spectrum of the protein near pH 13 is very similar to that of the fully unfolded state in 5 M GuHCl at pH 12 and 25°C. This observation suggests that the second base-induced conformational transition of EqTxII (between pH 11 and 13) is accompanied by a further disruption of tertiary structure. In fact, at pH 13, the base-induced denatured state of EqTxII retains very little tertiary structure, if any.

Inspection of Fig. 3b and Fig. 5b reveals that, between pH 7 and 10 (the first transition), the overall shape of the far UV CD spectrum of EqTxII remains essentially unchanged, even though the CD signal slightly decreases in magnitude. Thus, we conclude that, around pH 10, EqTxII essentially retains its native-like secondary structure although it may lack its native tertiary structure. Our analysis of the far UV CD spectrum of EqTxII in Fig. 3b revels that, at pH 10.3, the toxin has $10 \pm 1\%$ α-helical structure, $51 \pm 5\%$ β-structure, and $39 \pm 3\%$ aperiodic secondary structure. Note that, within experimental error, these numbers are quite similar to those for the native state of the toxin around pH 6 ($12 \pm 1\%$ α-helical structure, $52 \pm 5\%$ β-structure, and $36 \pm 3\%$ aperiodic secondary structure).

No further changes in the far UV CD spectrum occur between pH 10 and 11. However, an increase in the solution pH above pH 11 (the sec-

ond base-induced transition) results in an abrupt alteration of the shape and intensity of the far UV CD spectrum of the toxin. In particular, a new minimum appears at 208 nm (see Fig. 3b), which is suggestive of the protein being transformed into a state with a larger α-helical content [22]. Our analysis of the far UV CD spectrum of EqTxII in Fig. 3b revels that, at pH 13.3, the toxin has $54 \pm 3\%$ α-helical structure, $40 \pm 5\%$ β-structure, and only $6 \pm 3\%$ aperiodic secondary structure. Significantly, the switch from native-like secondary structure of EqTxII to non-native, α-helix enriched structure at pH 13 coincides with the complete loss of tertiary structure (see Fig. 3a). Thus, at pH 13, EqTxII lacks rigid tertiary structure but exhibits enhanced α-helical secondary structure.

Inspection of Fig. 4 reveals that, when the solution pH decreases from pH 13.3 to 10.8, the base-induced denatured state of EqTxII refolds into a new partially folded intermediate state, which spectroscopically resembles the state observed at acidic pH. However, further acidification of the solution to pH 1.3 does not result in further refolding of this partially folded intermediate. Consequently, the base-induced conformational transitions of EqTxII are virtually irreversible.

We have noticed that the acid- and base-induced denatured states of EqTxII have certain features in common. Most notable amongst these are the collapsed tertiary structures, as reflected in the near UV CD spectra (see Fig. 1a and Fig. 3a), and the non-native α-helix enriched secondary structures, as reflected in the far UV CD spectra (see Fig. 1b and Fig. 3b). However, the final base-induced denatured state of EqTxII at pH 13 is characterized by a significantly larger α-helical content ($54 \pm 3\%$) compared to the acid-induced denatured state at pH 1 ($19 \pm 1\%$) or the base-induced intermediate state at pH 11 ($10 \pm 1\%$).

4.2.2. Oligomerization of the base-induced denatured state of EqTxII

Inspection of our PAGE results presented in Fig. 8 reveals that, at 25°C, the base-induced denatured states of EqTxII above pH 12 oligomerize and form high molecular weight, water-soluble aggregates. Analogous to the acid-induced denatured state of EqTxII, one may propose that protein aggregation at highly alkaline pH may be responsible, at least in part, for the formation of non-native α-helix enriched secondary structure of the base-induced denatured state of the toxin.

As mentioned above, no protein band is observed on the PAGE gel for the base-induced denatured state of EqTxII at pH 12.6 at elevated temperatures. This observation suggests that, at elevated temperatures (95°C and, perhaps, lower) and highly alkaline pH, hydrolysis of the polypeptide chain of EqTxII is likely to occur.

Finally, a number of investigators have observed that pore formation by actinoporins involves the association of three to four toxin molecules (oligomerization) [4,45–48]. However, our results suggest that oligomeric EqTxII structures obtained at acidic pH (pH 1.2), alkaline pH (pH 12.6), or elevated temperatures (95°C) are significantly less active hemolytically than the native monomeric state of the toxin obtained under physiological solution conditions. Thus, the most biologically active form of EqTxII appears to be monomeric even though pore formation requires the toxin association into oligomers. This suggests that both the native monomeric conformation and interaction with the membrane are necessary for pore formation and hemolysis. Perhaps, the oligomerization of EqTxII molecules, required for performing their pore-forming function, occurs at the water–lipid interface or within the non-aqueous environment inside the membrane.

5. Conclusion

We have studied the conformational transitions of EqTxII using CD spectroscopy, ultrasonic velocimetry, high precision densimetry, viscometry, gel electrophoresis, and hemolytic activity assays. Depending on the environmental conditions, EqTxII may adopt various conformational states. At neutral pH and room temperature, the protein assumes a monomeric native state with rigid tertiary structure and predominantly β-sheet sec-

ondary structure. At acidic pH (below pH 2) and room temperature, the protein is irreversibly converted into a partially unfolded oligomeric state with disrupted tertiary structure and enhanced, non-native α-helical secondary structure. The acid-induced denatured state of EqTxII exhibits significantly reduced specific partial adiabatic compressibility and enhanced intrinsic viscosity compared to the native state. At elevated temperatures (above 50°C), the acid-induced denatured state of EqTxII reversibly denatures to a more unfolded state with decreased α-helical secondary structure.

At alkaline pH and room temperature, EqTxII undergoes two irreversible base-induced transitions. The first transition (between pH 7 and 10) results in a partial disruption of tertiary structure, while the secondary structure remains largely preserved. The second transition (between pH 11 and 13) is accompanied by a further disruption of tertiary structure and formation of extensive, non-native α-helical secondary structure. Analogous to the acid-induced denatured state of EqTxII at pH 1, the final base-induced denatured state at pH 13 forms large water-soluble aggregates.

In general, our results provide an experimental basis for a better understanding of mechanisms of biological toxicity of EqTxII and other pore-forming proteins. In particular, our results provide insight into the role of oligomerization and structural alterations of toxin molecules in modulating their pore-forming function.

Acknowledgements

The authors would like to thank the reviewer of the manuscript for his valuable comments concerning microscopic interpretations of the spectroscopic data. This work was supported by Slovene Science Foundation (ZIT-0003-97 and PZIT-0029-98 to N.P.) and NATO Collaborative Linkage Grant (LST.CLG 974812 to T.V.C).

References

[1] E. Gouaux, Channel-forming toxins: tales of transformation, Curr. Opin. Struct. Biol. 7 (1997) 697–701.

[2] P. Maček, D. Lebez, Kinetics of hemolysis induced by equinatoxin, a cytolitictoxin from sea anemone *Actinia equina*. Effect of some ions and pH, Toxicon 26 (1988) 441–445.

[3] N. Poklar, J. Lah, M. Salobir, P. Maček, G. Vesnaver, pH and temperature-induced molten-globule like denatured states of equinatoxin II: A study by UV-melting, DSC, far- and near-UV CD spectroscopy, and ANS fluorescence, Biochemistry 36 (1997) 14345–14352.

[4] G. Belmonte, G. Menestrina, C. Pederzolli et al., Primary and secondary structure of a pore-forming toxin from the sea anemone, *Actinia equina* L., and its association with lipid vesicles, Biochim. Biophys. Acta 1192 (1994) 197–204.

[5] M. Malavašič, N. Poklar, P. Maček, G. Vesnaver, Fluorescence studies of the effect of pH, guanidine hydrochloride and urea on equinatoxin II conformation, Biochim. Biophys. Acta 1280 (1996) 65–72.

[6] N. Poklar, J. Fritz, P. Maček, G. Vesnaver, T.V. Chalikian, Equinatoxin interactions with model lipid membranes: a calorimetric and spectroscopic study, Biochemistry 38 (1999) 14999–15008.

[7] F. Eggers, Th. Funck, Ultrasonic measurements with millilitre liquid samples in the 0.5–100 MHz range, Rev. Sci. Instrum. 44 (1973) 969–978.

[8] A.P. Sarvazyan, Development of methods of precise ultrasonic measurements in small volumes of liquids, Ultrasonics 20 (1982) 151–154.

[9] F. Eggers, Ultrasonic velocity and attenuation measurements in liquids with resonator, extending the MHz frequency range, Acustica 76 (1992) 231–240.

[10] A.P. Sarvazyan, E.E. Selkov, T.V. Chalikian, Constant-path acoustic interferometer with transition layers for precision measurements in small liquid volumes, Sov. Phys. Acoust. 34 (1988) 631–634.

[11] A.P. Sarvazyan, T.V. Chalikian, Theoretical analysis of an ultrasonic interferometer for precise measurements at high pressures, Ultrasonics 29 (1991) 119–124.

[12] D.W. Kupke, Physical principles and techniques of protein chemistry, in: S.J. Loch (Ed.), Density and Volume Change Measurements, Part C, Academic Press, New York, London, 1973, pp. 1–75.

[13] T.V. Chalikian, V.S. Gindikin, K.J. Breslauer, Volumetric characterization of the native, molten globule and unfolded states of cytochrome *c* at acid pH, J. Mol. Biol. 250 (1995) 291–306.

[14] S. Barnatt, The velocity of sound in electrolytic solutions, J. Chem. Phys. 20 (1952) 278–279.

[15] C. Pederzolli, G. Belmonte, M. Dalla Serra, P. Maček, G. Menestrina, Biochemical and cytotoxic properties of conjugates of tranferrin with equinatoxin II, a cytolysin from sea anemone, Bioconjugate Chem 6 (1995) 166–173.

[16] K. Gekko, Y. Hasegawa, Compressibility–structure relationship of globular proteins, Biochemistry 25 (1986) 6563–6571.

[17] K. Gekko, H. Noguchi, Compressibility of globular pro-

teins in water at 25°C, J. Phys. Chem. 83 (1979) 2706–2714.
[18] T.V. Chalikian, M. Totrov, R.A. Abagyan, K.J. Breslauer, The hydration of the globular proteins as derived from volume and compressibility measurements. Cross-correlating thermodynamics and structural data, J. Mol. Biol. 260 (1996) 588–603.
[19] S.E. Harding, The intrinsic viscosity of biological macromolecules. Progress in measurement interpretation and application to structure in dilute solution, Prog. Biophys. Molec. Biol. 68 (1997) 207–262.
[20] G. Anderluh, A. Barlič, Z. Podlesek et al., Cysteine-scanning mutagenesis of an eukaryotic pore-forming toxin from sea anemone: topology in lipid membranes, Eur. J. Biochem. 263 (1999) 128–236.
[21] S.W. Provencher, J. Glöckner, Estimation of globular protein secondary structure from circular dichroism, Biochemistry 20 (1981) 33–37.
[22] S.Y. Venyaminov, I.A. Baikalov, Z.M. Shen, C.-S.C. Wu, J.T. Yang, Circular dichroic analysis of denatured proteins: inclusion of denatured proteins in the reference set, Anal. Biochem. 214 (1993) 12–24.
[23] A.P. Sarvazyan, Ultrasonic velocimetry of biological compounds, Annu. Rev. Biophys. Biophys. Chem. 20 (1991) 321–342.
[24] T.V. Chalikian, A.P. Sarvazyan, K.J. Breslauer, Hydration and partial compressibility of biological compounds, Biophys. Chem. 51 (1994) 89–109.
[25] T.V. Chalikian, K.J. Breslauer, Thermodynamic analysis of biomolecules: a volumetric approach, Curr. Opin. Struct. Biol. 8 (1998) 657–664.
[26] T.V. Chalikian, K.J. Breslauer, Compressibility as a means to detect and characterize globular protein states, Proc. Natl. Acad. Sci. USA 93 (1996) 1012–1014.
[27] T.V. Chalikian, K.J. Breslauer, On volume changes accompanying conformational transitions of biopolymers, Biopolymers 39 (1996) 619–626.
[28] R. Filfil, T.V. Chalikian, Volumetric and spectroscopic characterization of the native and acid-induced denatured states of staphylococcal nuclease, J. Mol. Biol. 299 (2000) 827–842.
[29] A.P. Sarvazyan, P. Hemmes, Relaxational contributions to protein compressibility from ultrasonic data, Biopolymers 18 (1979) 3015–3024.
[30] T.V. Chalikian, D.P. Kharakoz, A.P. Sarvazyan et al., Ultrasonic study of proton-transfer reactions in aqueous solutions of amino acids, J. Phys. Chem. 96 (1992) 876–883.
[31] T.V. Chalikian, V.S. Gindikin, K.J. Breslauer, Spectroscopic and volumetric investigation of cytochrome *c* unfolding at alkaline pH: Characterization of the base-induced unfolded state at 25°C, FASEB J. 10 (1996) 164–170.
[32] T.V. Chalikian, V.S. Gindikin, K.J. Breslauer, Hydration of diglycyl tripeptides with non-polar side chains: a volumetric study, Biophys. Chem. 75 (1998) 57–72.
[33] L.R. Murphy, N. Matubaysi, V.A. Payne, R.M. Levy, Protein hydration and unfolding — insights from experimental partial specific volumes and unfolded protein models, Fold. Des. 3 (1998) 105–118.
[34] L.O. Narhi, J.S. Philo, T. Li, M. Zhang, B. Samal, T. Arakawa, Induction of α-helix in the β-sheet protein tumor necrosis factor-α: acid-induced denaturation, Biochemistry 35 (1996) 11454–11460.
[35] T. Sivaraman, T.K.S. Kumar, G. Jayaraman, C.C. Han, C. Yu, Characterization of a partially structured state in an all-β-sheet protein, Biochem. J. 321 (1997) 457–464.
[36] C. Tanford, Protein denaturation. Parts A and B, Adv. Protein Chem. 23 (1968) 121–282.
[37] C. Tanford, Protein denaturation, Part C, Adv. Protein Chem. 24 (1970) 1–95.
[38] A.L. Fink, Compact intermediate states in protein folding, Annu. Rev. Biophys. Biomol. Struct. 24 (1995) 495–522.
[39] D. Shortle, Denatured states of proteins and their roles in folding and stability, Curr. Opin. Struct. Biol. 3 (1993) 66–74.
[40] O.B. Ptitsyn, Molten globule and protein folding, Adv. Protein Chem. 47 (1995) 83–229.
[41] V.N. Uversky, D.J. Segel, S. Doniach, A.L. Fink, Association-induced folding of globular proteins, Proc. Natl. Acad. Sci. USA 95 (1998) 5480–5483.
[42] V.N. Uversky, A.S. Karnoup, R. Khurana, D.J. Segel, S. Doniach, A.L. Fink, Association of partially-folded intermediates of staphylococcal nuclease induces structure and stability, Protein Sci. 8 (1999) 161–173.
[43] K. Ramalingam, S. Aimoto, J. Bello, Conformational studies of anionic melittin analogues: effect of peptide concentration pH, ionic strength, and temperature-models for protein folding and halophillic proteins, Biopolymers 32 (1992) 981–992.
[44] R. Barker, Organic Chemistry of Biological Compounds, Prentice-Hall, Inc, Englewood Cliffs, New Jersey, USA, 1971.
[45] D.W. Michaels, Membrane damage by a toxin from the sea anemone *Stoichactis heliantus*. I. Formation of transmembrane channels in lipid bilayers, Biochim. Biophys. Acta 555 (1979) 67–78.
[46] W. Varanda, A. Finkelstein, Ion and nonelectrolyte permeability properties of channels formed in planar lipid bilayer membranes by cytolytic toxin from the sea anemone, *Stoichactis heliantus*, J. Memb. Biol. 55 (1980) 203–211.
[47] R. Zorec, M. Tester, P. Maček, W.T. Mason, Cytotoxicity of equinatoxin II from the sea anemone *Actinia equina* involves ion channel formation and an increase in intracellular calcium activity, J. Membrane Biol. 118 (1990) 243–249.
[48] M. Tejuca, M. Dalla Serra, M. Ferreras, M.E. Lanio, G. Menestrina, Mechanism of membrane permeabilization by sticholysin I, a cytolysin isolated from the venom of the sea anemone *Stichodactyla heliantus*, Biochemistry 35 (1996) 14947–14957.